$[Cyanil]_2^{2-}$ dimers possess long, two-electron ten-center ($2e^-/10c$) multicenter bonding†

Iñigo Garcia-Yoldi,[a] Joel S. Miller*[b] and Juan J. Novoa*[a]

Received 23rd April 2008, Accepted 29th May 2008
First published as an Advance Article on the web 5th June 2008
DOI: 10.1039/b806900j

A long, two-electron ten-center ($2e^-/10c$) [8 carbon plus 2 oxygen] bond in diamagnetic dimers of radical-anion tetracyano-1,4-benzoquinoneide (cyanil, $[Q]^{\bullet-}$), $[Q]_2^{2-}$, is described by B3LYP and CASSCF(2,2)/MCQDPT calculations.

Long, multi-center C–C bonds have been the focus of several recent studies with reduced tetracyanoethylene, TCNE, being the prototypical example.[1–6] $[TCNE]_2^{2-}$ π-dimers possess a long (~2.9 Å) C–C bond involving two electrons and four carbon atoms (Fig. 1a).[1–3] This bond results from the overlap of the $[TCNE]^-$ b_{2g} SOMOs to form b_{2u} $[TCNE]_2^{2-}$ bonding (Fig. 1b) and b_{1g} antibonding orbitals that are respectively doubly occupied and empty in the singlet ground state. This long C–C bond has the same electronic properties as conventional covalent bonds, except for its intrinsic energetic stability, which is mainly due to the cation$^+\cdots$[TCNE]$^{\bullet-}$ attractive interactions that overcome the anion–anion plus cation–cation repulsive interactions.[7]

In addition to $[TCNE]_2^{2-}$ other species exhibit sub-van der Waals separations suggestive of the presence of long, multicenter C–C bonding. Examples include anionic species, *e.g.* 7,7,8,8-tetracyano-*p*-quinodimethanide, $[TCNQ]^{\bullet-}$;[8] perfluoro-TCNQ $[TCNQF_4]^{\bullet-}$;[8,9] 2,3-dichloro-4,5-dicyanobenzo-quinonide, $[DDQ]^{\bullet-}$;[8,10] and tetracyano-1,4-benzoquinone {cyanil, $[Q]^{\bullet-}$};[11] cationic species, *e.g.* tetrathiafulvalenium, $[TTF]^+$;[12] tetramethylphenylenediaminium, $[TMPD]^+$;[13] and octamethylbiphenylenium;[14] as well as neutral radicals, *e.g.* substituted phenalenyl.[5,15] However, detailed analyses of the properties of the long C–C bonding in these π-dimers have yet to be reported, and thus the consequences of the larger size, aromatic nature *etc.* of the interacting fragments on the existence and properties of long C–C bonds have yet to be addressed. To gain a insight into these effects, here we report the electronic properties of the reduced cyanil π-dimers, $[Q]_2^{2-}$, obtained by combining B3LYP density functional, CASSCF(2,2) and CASSCF(2,2)/MCQDPT calculations at the crystal geometry of $[NEt_4]_2[Q]_2$.[11]

The $[NEt_4]^+$ and $[Fe(C_5Me_5)_2]^+$ salts of $[Q]^{\bullet-}$ form slipped, C_{2h} π-dimers, $[Q]_2^{2-}$ in the solid state that are displaced ~2.5 Å along the axis that contains the C–O bonds, and the average shortest intradimer C$\cdots$O and C$\cdots$C separations are 2.85 and 2.92 Å respectively.[11,16] These sub-van der Waals intradimer separations suggest the existence of some type of bonding interaction between the $[Q]^{\bullet-}$ moieties. The presence of this bond between the $[Q]^{\bullet-}$ moieties can be experimentally confirmed by solid-state magnetic susceptibility studies[11] that indicate that $[Q]_2^{2-}$ is diamagnetic, and also by solid-state electron paramagnetic resonance (EPR) studies that concluded that $[Q]_2^{2-}$ has a singlet ground state 8.8 kcal mol^{-1} below the triplet state.[17] Therefore the long bond found in $[Q]_2^{2-}$ has the same electronic properties as conventional bonds, and has all the features of the long, intradimer bond found in $[TCNE]_2^{2-}$.

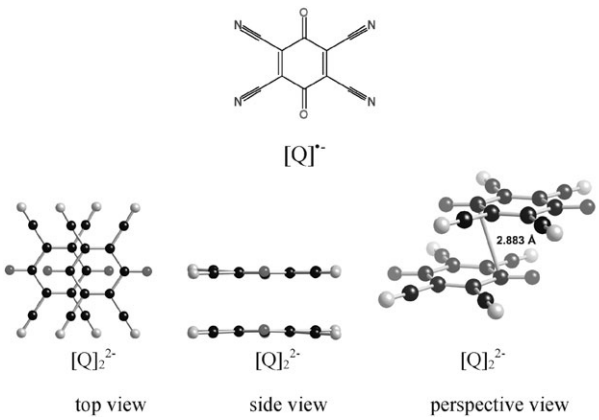

The non-conventional nature of the long bond between the $[Q]^{\bullet-}$ moieties of $[Q]_2^{2-}$ is revealed by showing that the $[Q]^{\bullet-}\cdots[Q]^{\bullet-}$ interaction is energetically repulsive. The interaction energy computed at the B3LYP/6-31 + G(d) level for an isolated C_{2h} $[Q]_2^{2-}$, present for $[NEt_4]_2[Q]_2$, is always repulsive (Fig. 2).[18] As occurs for $[TCNE]_2^{2-}$, a metastable minimum is

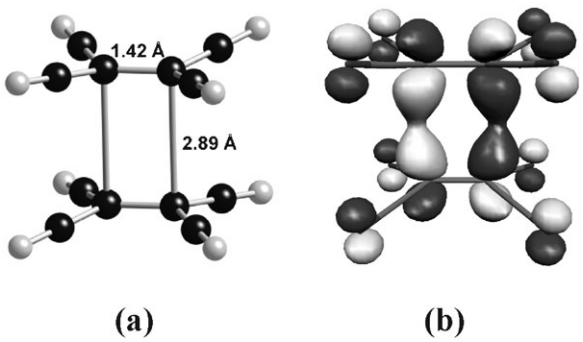

Fig. 1 Structure (a) and bonding (b) $2e^-/4c$ b_{2u} HOMO of the π-$[TCNE]_2^{2-}$ dimer.[1,2]

[a] *Departament de Química Física & IQTCUB Facultat de Química, Universitat de Barcelona, Av. Diagona, l647, 08028 Barcelona, Spain. E-mail: juan.novoa@ub.edu; Fax: 34 93 402 1231; Tel: 34 93 402 1228*
[b] *Department of Chemistry, University of Utah, Salt Lake City, Utah, 84112-0850, USA. E-mail: jsmiller@chem.utah.edu*

† Electronic supplementary information (ESI) available: Variation of the plot of the expectation value of $\hat{S}^2$ with the interfragment distance, shape of the orbitals in the (2,2) active space, geometry of the $[NEt_4^+]_2[cyanil^-]_2$ aggregate (coordinates and graph), and characteristics of the bond critical points. See DOI: 10.1039/b806900j

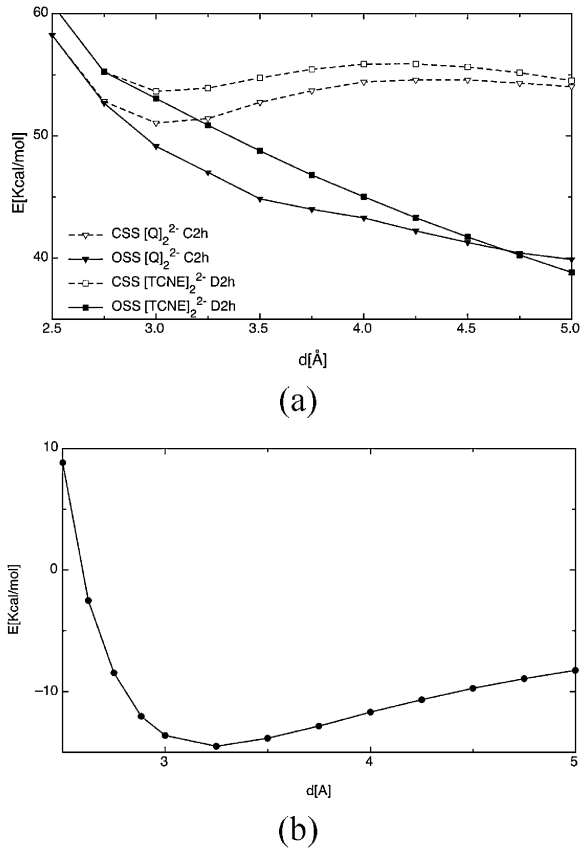

Fig. 2 (a) Potential energy curve (as a function of the shortest interfragment C···C distance, *d*, computed at the RB3LYP/6-31 + G(d) and UB3LYP/6-31 + G(d) levels for the CSS and OSS states of the C_{2h} $[Q]_2^{2-}$ and D_{2h} $[TCNE]_2^{2-}$ dimers (all curves dissociate into two radical–anions). (b) Potential energy curve for the dissociation of a $[NEt_4]_2[Q]_2$ aggregate into two ($[NEt_4]^+\cdots[Q]^-$) units, computed at the UB3LYP/6-31 + G(d) level.

found at the RB3LYP level for the closed-shell singlet (CSS) state. However, the metastable minimum disappears at the UB3LYP level where the singlet has a non-negligible open-shell nature which becomes more important as the intradimer distance increases. For C···C = 3.0 Å the UB3LYP natural orbital population has occupation numbers of 1.59 and 0.61 for the HOMO and LUMO orbitals, respectively, and the expectation value of $\hat{S}^2$ is 0.66, but both occupation numbers become almost 1.0 above 4 Å, where the expectation value of $\hat{S}^2$ also becomes 1.0 (Fig. S1† shows the variation of the expectation value of $\hat{S}^2$ for the Fig. 2a and b UB3LYP curves; for the RB3LYP curves $\hat{S}^2 = 0$ everywhere). Thus, the singlet computed at the UB3LYP level is mostly an open-shell singlet (OSS),[19] which only becomes a CSS close to 2.5 Å (see Fig. S1†). Note that the UB3LYP interaction energy curve for lowest energy triplet state is nearly degenerate with that for OSS. Finally, at the same distance and method, the $[TCNE]_2^{2-}$ curves are lower in energy than those for $[Q]_2^{2-}$. This is attributed to the greater energy required by the $[Q]^{\bullet-}$ to bend, due to its ring structure.

If the $[Q]^{\bullet-}\cdots[Q]^{\bullet-}$ interaction is energetically repulsive, why are there short (2.883 Å) $[Q]_2^{2-}$ intradimer separations? Similar to that shown for the $[TCNE]_2^{2-}$ dimers, their existence can be mostly attributed to the attractive cation$^+\cdots[Q]_2^{2-}$ interactions exceeding the anion–anion and cation–cation repulsive interactions. This fact can be already manifested in $[NEt_4]_2[Q]_2$ aggregates found in the crystal, which can be seen as the minimum units from which the crystal is generated after applying various symmetry operations. At their crystal geometry the interaction energy computed for these aggregates is −124.4 kcal mol^{-1} at the RB3LYP/6-31 + G(d) and UB3LYP/6-31 + G(d) levels, which becomes −120.5 kcal mol^{-1} after correcting the basis-set superposition error (BSSE) using the counterpoise method.[20] The stabilizing nature of the interaction energy results from adding the four attractive $[NEt_4]^+\cdots[Q]^{\bullet-}$ interactions (−56.2, −51.8, −51.8 and −56.0 kcal mol^{-1}) and the repulsive $[NEt_4]^+\cdots[NEt_4]^+$ and $[Q]^{\bullet-}\cdots[Q]^{\bullet-}$ interactions (27.0 and 55.0 kcal mol^{-1} respectively). Note that the singlet is closed-shell in the RB3LYP calculations while, as noted above, it is has a non-negligible open-shell character in the UB3LYP calculations. The stability of a $[NEt_4]_2[Q]_2$ aggregate can be further noted by fully optimizing its geometry at the RB3LYP or UB3LYP levels (a minimum was found at the RB3LYP level in which the optimum intradimer C···C distance is 3.064 Å). It can also be seen by looking at the UB3LYP potential-energy curve for its dissociation into two $[NEt_4]^+\cdots[Q]^{\bullet-}$ units, see Fig. 2b.

The stability of the $[NEt_4]_2[Q]_2$ aggregate explains the intradimer bonding despite the repulsive nature of the $[Q]^{\bullet-}\cdots[Q]^{\bullet-}$ interaction and their long distance. At 2.883 Å the SOMO orbitals of the two $[Q]^{\bullet-}$ moieties overlap to form bonding and antibonding MOs (Fig. 3), and the bonding orbital becomes doubly occupied in the ground-state singlet, as for conventional covalent bonds. This explains the observed diamagnetism of the $[Q]_2^{2-}$ dimers. Note that in the bonding orbital the two SOMO orbitals overlap *via* five in-phase components (*i.e.* ten centers) to make three in-phase C···C and two in-phase C···O overlaps. This indicates that the long bond present in these $[Q]_2^{2-}$ dimers is a 2-electron/10-center bond.

It was also observed[21] in π-$[TCNE]_2^{2-}$ dimers that part of the stability of cation$_2$[TCNE]$_2$ aggregates originated from correlation interactions that cannot be described at the B3LYP level, but are properly described at the CASSCF(2,2)/MCQDPT level. Therefore, CASSCF(2,2)/MCQDPT calculations were also performed for the $[NEt_4]_2[Q]_2$ aggregates, using the 6-31 + G(d) basis set and the active space shown in Fig. S3 (the bonding and antibonding combinations of the SOMO orbitals of $[Q]^{\bullet-}$).† Due to computational restrictions they were carried out by substituting the $[NEt_4]^+$ cations by K^+ placed in the position of the N and maintaining $[Q]_2^{2-}$ in the same location. The resulting $K_2[Q]_2$ aggregates have a CASSCF(2,2)/MCQDPT interaction energy of −92.4 kcal mol^{-1}, of the order of that reported above at the B3LYP level for the $[NEt_4]_2[Q]_2$ aggregates. The reduced stability is due to the non-optimum position of the K^+ cations, as noted by the UB3LYP interaction energy of the $K_2[Q]_2$ aggregates being −117.1 kcal mol^{-1}. As also found for $[TCNE]_2^{2-}$ at the CASSCF(2,2)/MCQDPT level, the ground state for $[Q]_2^{2-}$ is a closed-singlet state in agreement with

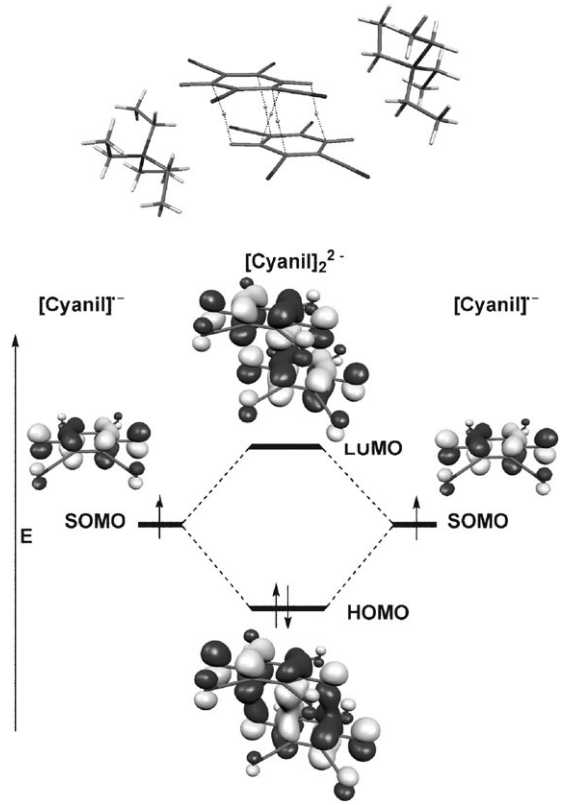

Fig. 3 Geometry of the $[NEt_4]_2Q_2$ aggregate indicating the (3,−1) bond critical points and atoms bonded (top). MO diagram showing how the SOMO orbitals of $[Q]^{\bullet -}$ combine to generate the $[Q]_2^{2-}$ dimer bonding and antibonding orbitals (bottom). In the ground, closed-shell singlet state of the dimer the bonding orbital is the double occupied HOMO.

$[NEt_4]_2[Q]_2$ being diamagnetic. This diamagnetism is not found from the UB3LYP calculations at the crystal geometry (as seen in Fig. 1, the OSS is more stable than the CSS at the aggregate crystal geometry).

The characteristics of the long C–C bonds formed within the $[Q]_2^{2-}$ were finally investigated by atoms-in-molecules[22] (AIM) calculations (Tables S1–S2 and Fig. S2†). An AIM analysis of the (3,−1) bond critical points in the aggregate was done on the RB3LYP wavefunction, as this is the wavefunction that corresponds to the experimental singlet ground state and is the best theoretical method. It shows five bond critical points: two C···O and three C···C. Thus, the long bond involves two electrons and 10 centers, 8 C and 2 O.

Thus, the analysis of the observed sub van der Waals interactions for $[Q]_2^{2-}$ and the deviations from planarity for the $[Q]^{\bullet -}$ moieties obtained in the RB3LYP optimizations and the analysis of the qualitative MO diagram obtained from B3LYP and CASSCF(2,2)/MCQDPT calculations reveal intradimer bonding between the $[Q]_2^{2-}$ fragments at a distance of 2.883 Å in accord with that observed for π-$[TCNE]_2^{2-}$. In addition to the orbital overlap and correlation, the stability of this unconventional intradimer $[Q]_2^{2-}$ bond also comes from the cation···anion interactions, whose sum must exceed the sum or repulsive electrostatic interactions. At 2.883 Å, the SOMO orbitals of the two $[Q]^{\bullet -}$ moieties overlap to form bonding and antibonding MOs (Fig. 3) with five components, 3 C···C and 2 C···O, in agreement with the results of AIM calculations. This overlap explains the observed diamagnetism of the $[Q]_2^{2-}$ dimers, and similar bonding occurs for $[chloranil]_2^{2-}$ and $[2,3\text{-dichloro-}5,6\text{-dicyanobenzoquinone}]_2^{2-}$, and it is also similar to that found in conventional covalent bonds.

Acknowledgements

IG-Y and JJN were supported by the Spanish Science and Education Ministry (BQU2002-04587-C02-02 and UNBA05-33-001, and PhD grant to IG-Y) and the CIRIT (2001SGR-0044 and 2005-PEIR-0051/69). Computer time was also provided by CESCA and BSC. JSM was supported in part by the US NSF (Grant No. 0553573), the US DOE (Grant No. DE FG 03-93ER45504).

References

1. J. J. Novoa, P. Lafuente, R. E. Del Sesto and J. S. Miller, *Angew. Chem., Int. Ed.*, 2001, **40**, 2540; R. E. Del Sesto, J. S. Miller, J. J. Novoa and P. Lafuente, *Chem.–Eur. J.*, 2002, **8**, 4894; J. J. Novoa, P. Lafuente, R. E. Del Sesto and J. S. Miller, *CrystEngComm*, 2002, **4**, 373.
2. J.-M. Lu, S. V. Rosokha and J. K. Kochi, *J. Am. Chem. Soc.*, 2003, **125**, 12161; J. Jakowski and J. Simons, *J. Am. Chem. Soc.*, 2003, **125**, 16089; Y. Jung and M. Head-Gordon, *Phys. Chem. Chem. Phys.*, 2004, **6**, 2008.
3. J. S. Miller and J. J. Novoa, *Acc. Chem. Res.*, 2007, **40**, 189.
4. J. D. Bagnato, W. W. Shum, M. Strohmeier, D. M. Grant, A. M. Arif and J. S. Miller, *Angew. Chem., Int. Ed.*, 2006, **45**, 5326.
5. G. Goto, T. Kubo, K. Yamamoto, S. K. Nakazawa, K. Sato, D. Shiomi, T. Takui, M. Kubota, Y. Kobayshai, K. Yakusi and J. A. Ouyang, *J. Am. Chem. Soc.*, 1999, **121**, 1619.
6. I. Garcia-Yoldi, J. J. Novoa and J. S. Miller, *J. Phys. Chem. A*, 2007, **111**, 8020.
7. In addition there is also a smaller stabilization coming from the dispersion component. I. Garcia-Yoldi, F. Mota and J. J. Novoa, *J. Comput. Chem.*, 2007, **28**, 326.
8. *E.g.*: A. H. Reis, Jr, E. Gebert and J. S. Miller, *Inorg. Chem.*, 1981, **20**, 313; S. Z. Goldberg, B. Spivack, G. Stanley, R. Eisenberg, D. M. Braitsch, J. S. Miller and M. Abkowitz, *J. Am. Chem. Soc.*, 1977, **99**, 110; M. C. Grossel, F. A. Evans, J. A. Hriljac, K. Prout and S. C. Weston, *J. Chem. Soc., Chem. Commun.*, 1990, 1494; R. C. Hynes, J. R. Morton, K. F. Preston, A. J. Williams, F. Evans, M. C. Grossel, L. H. Sutcliffe and S. C. Weston, *J. Chem. Soc., Faraday Trans.*, 1991, **87**, 2229; T. Azcondo, L. Ballester, S. Golhen, A. Gutierrez, L. Ouahba, S. Yartsev and P. Delhaes, *J. Mater. Chem.*, 1999, **6**, 1237.
9. M. T. Johnson, A. M. Arif and J. S. Miller, *Eur. J. Inorg. Chem.*, 2000, 1781, and references therein.
10. *E.g.*: G. Zanotti, *Acta Crystallogr., Sect. B*, 1982, **38**, 1225; J. S. Miller, P. J. Krusic, D. A. Dixon, W. M. Reiff, J. H. Zhang, E. C. Anderson and A. J. Epstein, *J. Am. Chem. Soc.*, 1986, **108**, 4459; J. J. Mayerle and J. B. Torrance, *Bull. Chem. Soc. Jpn.*, 1981, **54**, 3170; A. Marzotto, D. A. Clemente and L. Pasimeni, *J. Crystallogr. Spectrosc. Res.*, 1988, **18**, 545.
11. C. Vazquez, J. C. Calabrese, D. A. Dixon and J. S. Miller, *J. Org. Chem.*, 1993, **58**, 65.
12. *E.g.*: B. A. Scott, S. J. La Placa, J. B. Torrance, B. D. Silverman and B. T. Welber, *J. Am. Chem. Soc.*, 1977, **99**, 6631.
13. *E.g.*: M. J. Hove, B. M. Hoffman and J. Ibers, *J. Phys. Chem.*, 1972, **56**, 3490; J. Tanaka and N. Sakabe, *Acta Crystallogr., Sect. B*, 1968, **24**, 1345; J. Tanaka, M. Inoue, M. Mizuno and K. Horai, *Bull. Chem. Soc. Jpn.*, 1970, **43**, 1998.
14. J. K. Kochi, R. Rathore and P. Le Magueres, *J. Org. Chem.*, 2000, **65**, 6826.
15. Y. Morita, J. Kawai, K. Fukui, S. Nakazawa, K. Sato, D. Shiomi, T. Takui and K. Nakasuji, *Org. Lett.*, 2003, **5**, 3289.
16. The shortest intradimer C···O distances are 2.801 and 2.908 Å for the $[NEt_4]^+$ and $[Fe(C_5Me_5)_2]^+$ salts respectively, likewise the

shortest intradimer C···C distances are 2.883 and 2.944 Å, and the shortest spacings between the parallel (O)CC(O) lines are 2.72 and 2.76 Å.
17. R. C. Hynes, P. J. Krusic, K. F. Preston, J. J. Springs, A. J. Williams and J. S. Miller, *J. Am. Chem. Soc.*, 1995, **117**, 2547.
18. At each point of the potential-energy curve, the geometry was optimized while preserving the cofacial conformation.
19. The OSS state was computed at the UB3LYP level by using the broken symmetry approach, which is known to give a good description of the relative stability of these states in HF and DFT calculations. See: L. Noodleman, *J. Chem. Phys.*, 1981, **74**, 5737; L. Noodleman and E. Davidson, *Chem. Phys.*, 1986, **109**, 131.
20. S. F. Boys and F. Bernardi, *Mol. Phys.*, 1970, **19**, 553.
21. I. Garcia-Yoldi, F. Mota and J. J. Novoa, *J. Comput. Chem.*, 2007, **28**, 326.
22. R. F. W. Bader, *Atoms in Molecules*, Oxford University Press, Oxford, UK, 1990.